Reliability Study of Micro-Pin Fin Array for On-Chip Cooling

David C. Woodrum, Thomas Sarvey, Muhannad S. Bakir, Suresh K. Sitaraman*
Georgia Institute of Technology
Atlanta, GA, U.S.A. 30332
*Email: suresh.sitaraman@me.gatech.edu

Abstract

With continued power, performance, functionality, and miniaturization demands, microelectronic devices can dissipate upwards of 50 W/cm^2 reaching to 100's of W/cm^2 and possibly 1000 W/cm^2 in the next 10 years. With such a high heat flux, traditional cooling through thermal interface material and heat spreader may not be able to remove the heat, especially from hot spots. In an ongoing research at Georgia Tech, innovative fluid-thermal solutions are being pursued where deionized water or refrigerants are circulated through an array of micro-pin fins etched into the backside of the silicon. In the proposed configuration, the thick backside of the silicon is used to etch an array of micro-pin fins and the silicon die is then bonded to another silicon or quartz substrate to create a micro-pin fin channel for fluid flow. To maximize heat flux, the fluid is expected to be in two-phase. The objective of this paper is to examine such a micro-pin fin array from the standpoint of cracking and reliability.

Introduction

Utilization of on-chip fluidic cooling techniques is a growing area of interest for maintaining reasonable temperature ranges even in high heat flux applications [1]. Inherently, the design and implementation of fluidic microgap architectures introduces new pressure effects which can be detrimental to mechanical reliability. Thermal performance has been shown to improve for higher flow rates, which increases pressure drop across the device. Pressure requirements are further increased by adding pin fins which have consistently been shown to improve heat transfer metrics [2]. Maintaining higher overall pressures also allows for utilization of refrigerants under two-phase flow conditions, an optimal scenario from a thermal performance standpoint [3]. Failures during experimental work have occurred for internal pressures on the order of 700 kPa, a limit which is much lower than the intermediate and long term goals of 1500 and 3000 kPa respectively to achieve 1000 W/cm^2. Such pressure targets would facilitate heat removal using high-performance refrigerant fluids [3].

With thermal gradients, high fluid pressure, and wall shear stress, the micro-pins can crack and/or the silicon substrate or glass cap may crack. Fig. 1 shows the proposed configuration that has a silicon substrate with an array of micro-pin fins sandwiched between the silicon substrate and a capping glass layer. The silicon substrate and the glass capping layer are bonded to each other using epoxy that is dispensed around the periphery. The entire sample is about 30 mm long, 14 mm wide, and 1.3 mm thick. The fluid inlet and the outlet are etched into silicon substrate flowing through the channel of about 25 mm. Mechanical supports are also built in to be able to direct the flow toward the micro-pin array and provide overall support to the assembly. The array of pin fins, used to improve heat transfer rates, occupies the 1 cm^2 square region in the center. Also, a single row of flow distribution pins are fabricated to ensure uniform flow through the micro-pin array. Two pressure ports, not illustrated in Fig. 1, are also present in the assembly to measure the fluid pressure before and after the micro-pin fin array.

This work examines the cracking of the silicon, glass, and micro-pin fins. It is seen that when epoxy bonding is done, it is not always possible to bond all micro-pin fins to the upper cap, and thus the structure could fracture and fail due to internal fluid pressure as in Fig. 2. The top photograph is an as-assembled sample. As seen, the flow space between the glass cap and the silicon substrate is shaped like a trapezoid, and the central square area with a lighter color has the micro-pin fin array. The two pressure ports are also shown Fig. 2.

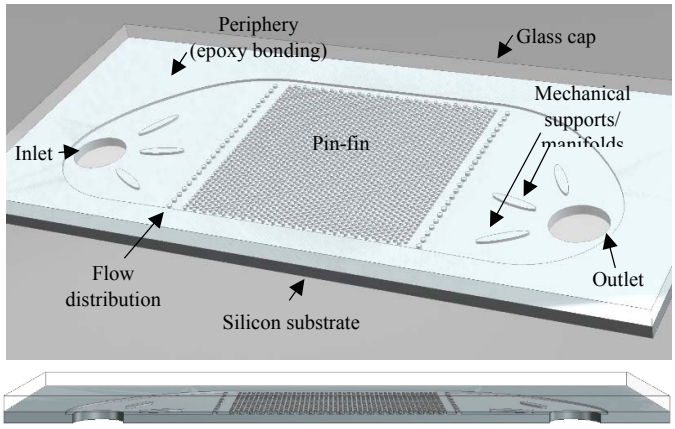

Fig. 1. Schematic of micro-pin fin assembly —isometric view (top), side view (bottom)

The bottom photograph in Fig. 2 shows a fractured sample, after fluid was injected at a high pressure. The thinned silicon side of the microgap has broken around the edges of the pin fin array, leaving only the glass cap on top. For contrast purposes, the broken sample was placed on a brown surface before being photograph. The glass capping layer is fully intact, the bottom silicon is broken wherever the brown surface is seen, and the bottom silicon is still adhered to the glass cap near the triangular areas where epoxy is present. This means that when the entire cavity is pressurized, the silicon flexes out and fractures. This failure mode is modeled and the results are discussed.

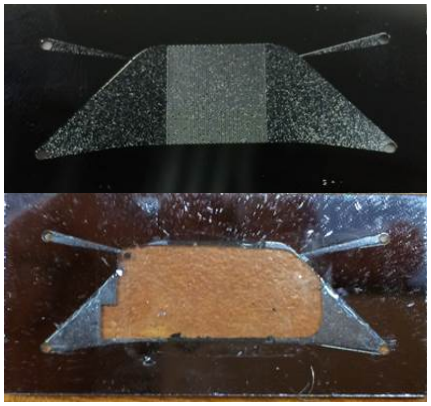

Fig. 2. Photograph of a working device (top) and fractured device after fluid pressure test (bottom)

Initial Modeling and Stress Results

Using ANSYS® Mechanical, a 3-D structural model is developed. The geometry is constructed using a bottom-up process for direct control of mesh density and geometry build-up. Areas are generated to form various geometric entities such as inlet/outlet ports, supports, flow distribution pins, and pin-fin array. These areas are meshed and then extruded out of plane to form a 3-D system of elements corresponding to the known architecture used in experiments.

In developing boundary conditions for this model, the bonding techniques are the primary consideration. Initial experimental tests are conducted on samples for which a 500 µm thick silicon is bonded to a 700 µm thick glass using epoxy. This process involves direct application of an epoxy compound to the large, flat region around the flow space, to be referred to as the device periphery. Fig. 3 lays out the processing steps for these devices, including the manual application of epoxy around the periphery. It is not possible to use manual epoxy bonding on the interior features of the microgap, such as the pin-fin heads and the mechanical supports, due to their relatively small size. The blue area in Fig. 4 illustrates the area where the two layers are bonded.

To study the pressure-induced failure, all faces of the flow space are subjected to the applied fluid pressure. A fixed condition is also applied on the far left edge of the geometry to prevent rigid body motion and rotation. The mating nodes at the bottom of the glass cap and the top of the silicon substrate are merged together where epoxy is present, and are not merged together where epoxy is not present. Thus, this condition simulates the case when epoxy bonding only occurs on the periphery of the device as illustrated in Fig 4. The necessary material properties and the assembly dimensions used in the simulations are given in Tables 1 and 2.

Based on this setup, the ANSYS model is solved. With the number of structural elements in excess of half a million and three translational degrees of freedom, the model requires approximately six hours to solve on a six-core processor. A mesh convergence is also conducted to ensure that the results have converged. The displacement contours are shown in Fig. 5. Due to the absence of bonding on the interior features, both the glass and silicon are allowed to flex. The maximum displacement occurs near the center of the silicon substrate.

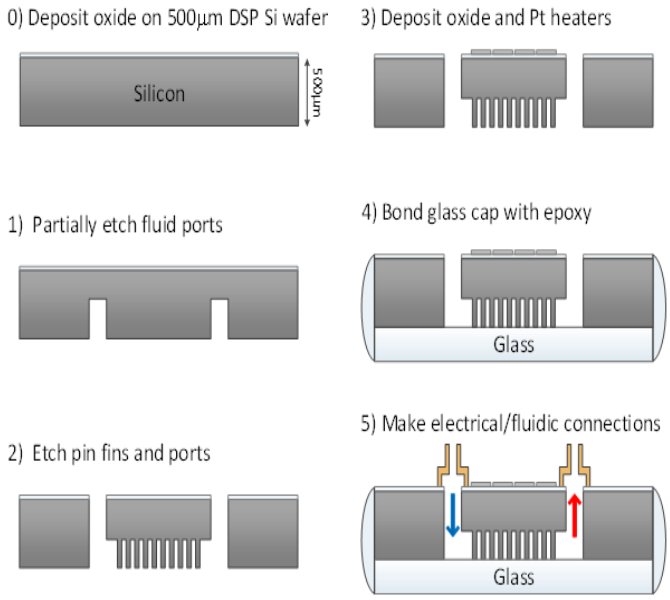

Fig. 3. Steps for device fabrication

This is due to the fact that the silicon substrate is thin and less rigid compared to the glass capping layer due to the etching of micro-pin fin array at the central area of silicon substrate, and the silicon substrate bends outward due to the applied normal pressure. The thick glass cap does not bend much due to its high flexural rigidity.

Stresses develop near the edge of the flow space due to this flexing action. The first principal stress contours are shown in Fig. 6. These results show that high internal pressure causes high bending stresses near the edges of the microgap, and the stress can be as high as 450 MPa near the edges of the silicon, when the fluid pressure is 700 kPa. As the fracture toughness of silicon is in the range of 0.7 to 1 MPa$\sqrt{m}$ [4], the silicon substrate will fracture at these high stresses considering a flaw size of about 0.7 µm due to processing or near the sharp corners at the edges. In general, it is seen through more than one sample that the epoxy bonded samples fracture around 700 kPa. Therefore, as an alternative, anodic bonding is tried where the silicon substrate and glass cap are bonded at high temperature, pressure, and voltage with the expectation all of the micro-pin fins, manifolds, and flow distribution pins will be bonded to the glass cap.

Experimental Techniques: Dye and Pry

TABLE 1: MATERIAL PROPERTIES

Parameter	Silicon	Glass
Material Model	Elastic Anisotropic	Elastic
Modulus, E	C_{11}:166 GPa C_{12}: 63 GPa C_{44}: 80 GPa	70 GPa
Poisson, ν	0.28	0.16

In order to verify the knowledge gained from finite-element modeling, experimental pressure tests are conducted using microgap samples fabricated by the method previously discussed. A dye-and-pry method is developed and utilized to visually evaluate the presence of any separation between glass cap and silicon substrate for a range of internal pressures. Dye-and-pry techniques are commonly used for determining cracks and defects in solder joints in microelectronic packages, e.g. [5], [6], where a dye is allowed to flow into solder joint cracks. When the dye is dried and the sample is pried open, the cracked areas are visible due to the presence of dried dye. A similar technique is used for the microfluidic sample assembly where a green working fluid, triarylmethane food dye, is pumped in using a syringe pump. The outlet of the device is sealed such that the system became a closed control volume. A pressure transducer measures the instantaneous static pressure of the system, while the microscope captures images of the pin fins and other features of the microgap. The syringe pump is gradually actuated by a mechanical clamp, compressing the liquid inside the closed loop. The goal of this test is to visually capture the pressure at which green working fluid fills any gap formed between the glass and silicon. Additional concerns with this test include fluid leakage, depth of field, levelness of the sample beneath the microscope, and safety of the working environment at failure point.

An image of the sample taken prior to the dye-and-pry test is shown in Fig. 7. As seen, the sample has an array of micro-pin fins with a diameter of 50 µm and larger flow distribution pins of 100 µm diameter. As the fluid pressure is gradually increased, the sample silicon breaks when the fluid pressure reaches 800 kPa. This maximum pressure exceeds the range of pressures previously seen for peripheral epoxy bonding, though it is still within 20% of the previously recorded values. Upon further examination and analysis, it is seen that the anodic bonding parameters employed in this experiment do not ensure that all of the micro-pins are bonded to the glass cap.

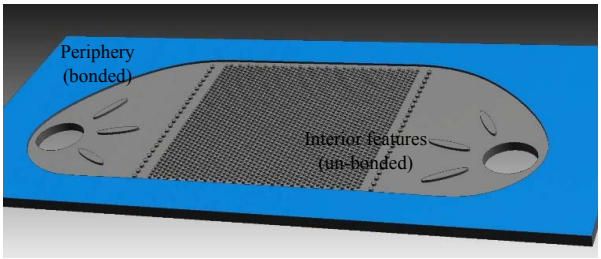

Fig. 4. Bonding of silicon and glass layers: periphery bonded (blue) but not interior

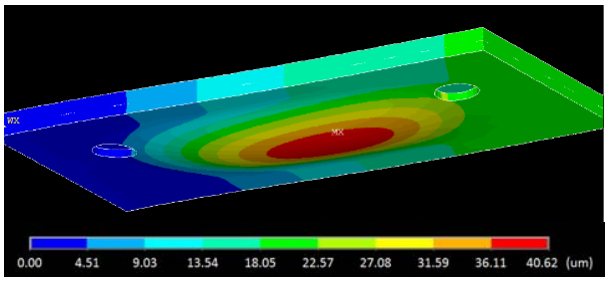

Fig. 5. View of maximum displacement on underside of silicon for peripheral bonding scenario; exaggerated visual

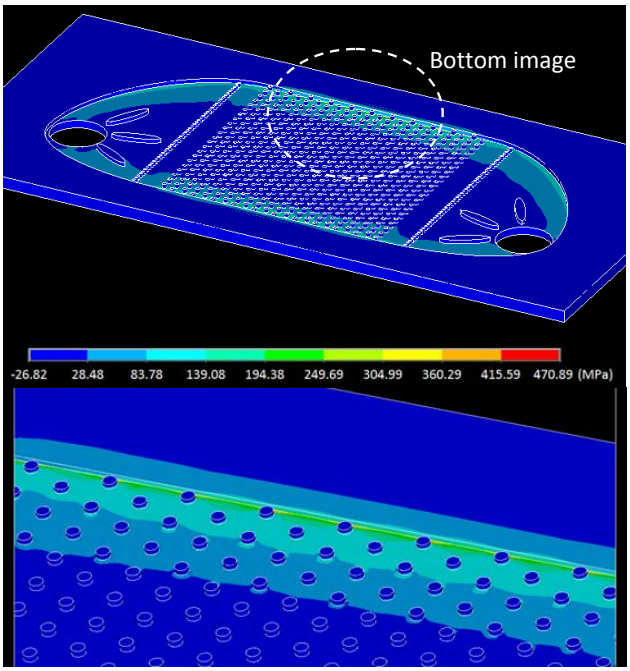

Fig. 6. Cut view of first principal stress in silicon side of model for peripheral bonding scenario; global view (top) and zoomed view of top silicon edge (bottom)

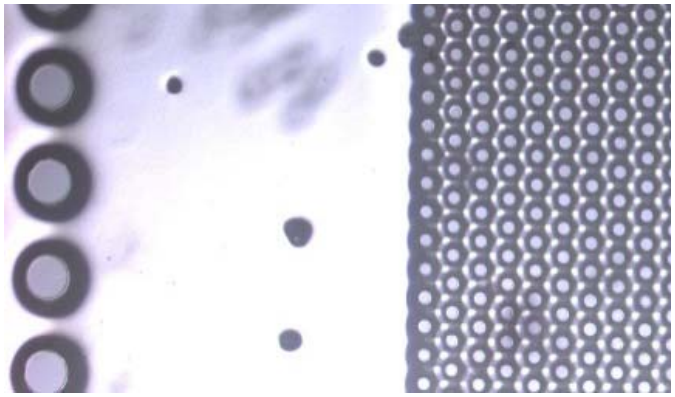

Fig. 7. As-fabricated-and-assembled sample before fluid pressure test

Post-Test Inspection and Results

Immediately after sample failure, the sample can be visually inspected using the same setup since the dye will emain in place and typically begin to dry. This reduces the risk of destroying the remainder of the sample due to handling. As illustrated in Fig. 8, sample fracture occurs around the periphery. In every case cracking develops around the peripheral edge of the microgap, mostly in the silicon side. For the case shown in Fig. 8, cracking takes place around the edges of both glass and silicon as well as the centerline of the silicon on the pin fin array. Half of the

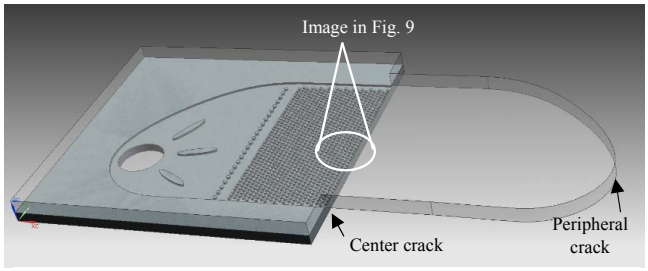

Fig. 8. Model of broken sample after attaining maximum pressure of 800 kPa

TABLE 2: GEOMETRIC PARAMETERS

Geometric Parameter	Value
L_chip	2.5 cm
W_chip	1.4 cm
D_pin	150 µm
P_pin	225 µm
L_array	1 cm
T_silicon	500 µm
T_glass	700 µm
H_gap_etch	100 µm

device remains fully intact—both silicon and glass are present, while the other half has broken off except for part of the glass cap. This sample presents a unique opportunity to view a section of the silicon pin-fin array which is still capped by glass, even after failure. Visualization of the flow space through the glass possible. One microscope image near the fracture zone is presented in Fig. 9.

As seen in Fig. 9, even after using air to purge the bulk of the green fluid from the system, dye is trapped between the glass cap and the top of the silicon pin fins. This suggests there is sufficient separation occurring during pressurization to allow fluid to fill the gap between the pin fin and glass. In addition, the intensity of the coloration is maximum for pin fins near the center of the device, nearest the crack zone. As you move away from the center of the package, the intensity is less. This indicates pins near the edges of the sample do not open as much as the pins near the center of the sample where the outward deflection is maximum due to fluid pressure. An image taken after drying of the trapped liquid is shown in Fig. 10. In this instance, the dye has dried fully as in a typical dye and pry test. Glass and silicon remain to the left of the crack, while glass is the only material present to the right. The coloration intensity on the pin-fin heads tapers off to the left of the crack. This intensity gradient may suggest smaller gap size and therefore less flexural deformation away from the crack zone, as is expected from the displacement results of finite-element modeling. The maximum pressure that is sustained during this experimental test, 800 kPa, does not meet the goal of 1500 kPa.

Modeling of Ideal Bonding Scenario

Based on experimental results, partial bonding of glass to silicon does not dramatically increase the pressure limit. Possibly through optimized anodic bonding, greater limits

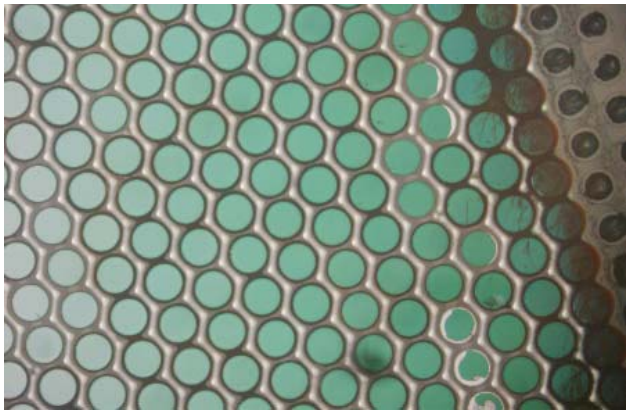

Fig. 9. 150 µm diameter pin-fin heads after fracture (still covered by glass)

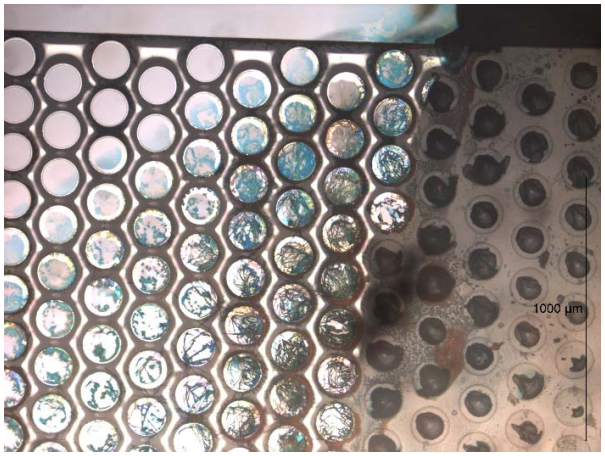

Fig. 10. Dried sample showing dried working fluid

can be achieved. If the bond strength between the top surfaces of the smaller interior features and the glass cap can be increased, an ideal scenario can be attained. In this ideal state, the unattached region would be reduced in size and constrained by the presence of these added mechanical supports. This could reduce the overall propensity for failure by decreasing the effective moment arm dramatically, alleviating stress at the corners.

Modeling this scenario essentially removes the unmerged nodes condition from the previously defined model setup. Thus, the top of the silicon pin fins and supports are assumed to be bonded to the glass cap, which is the ideal bonding scenario. This is demonstrated in Fig. 11.

Keeping all other conditions consistent, this model is solved and results are analyzed to determine first principal stress in silicon. Fig. 12 presents the stress contours of the ideal bonding case. The maximum principal stress reaches approximately 175 MPa, almost a 3 fold reduction compared to the peripheral bonding result of approximately 450 MPa. Displacements are also significantly reduced, with the locations of maximum deformation still occurring at the maximum distance from nearest support. As pressure correlates linearly with stress\, achieving ideal bonding should increase the achievable pressures to exceed 1500 kPa assuming failure still occurs at 450 MPa on the silicon side. Further consideration must be given to other failure modes,

particularly in the interface of anodic bonding and in the glass itself.

Based on this study, new designs and new anodic bonding parameters are being considered. For example, the manifolds and support sections will be made sufficiently larger and more such supports will be introduced to ensure that the top glass cap is adequately bonded to the silicon substrate. Selected micro-pins in the micro-pin fin array will be designed somewhat larger to ensure anodic bonding between the silicon substrate and the glass cap. Anodic bonding parameters will be reviewed to make sure that the intended surfaces are successfully bonded. Materials such as spin on glass will be considered to ensure that the height variations among different pins in the micro-pin fin array do not prevent some of the pins from bonding to the glass cap. These various future sample designs and processes will be tested in a similar manner to determine the effectiveness of anodic bonding and to predict the allowable pressure range of these devices.

Fig. 11. Bonded regions (blue) for ideal bonding scenario

Conclusion

The structural integrity of a silicon-glass micro-fluidic assembly is studied through experiments and simulations. It is seen that when epoxy is used around the periphery to bond the silicon and glass layers, the assembly cannot withstand more than 700 kPa of fluid pressure. When un-optimized anodic bonding is used, the assembly can withstand 800 kPa of fluid pressure which is still far less than the 1500 kPa of fluid pressure required for high heat-flux removal applications. New designs and modified anodic bonding parameters are being explored to create a design that can withstand close to 1500 kPa. Numerical simulations show such pressure targets are possible to achieve.

Acknowledgments

The authors gratefully acknowledge the financial support provided by DARPA through the IceCool Fundamentals Program (Award No. HR0011-13-2-0008).

References

1. Y. Zhang, A. Dembla, and M. S. Bakir, "Silicon micropin-fin heat sink with integrated TSVs for 3-D ICs: trade-off analysis and experimental testing," *IEEE Trans. Components, Packaging and Manufacturing Technology*, vol. 3, pp. 1842-1850, 2013.
2. P. M. Ligrani, M. M. Oliveira, and T. Blaskovich. "Comparison of Heat Transfer Augmentation Techniques", *AIAA Journal*, Vol. 41, No. 3 (2003), pp. 337-362.
3. P.A. Kottke, T.M. Yun, C.E. Green, Y.K Joshi, A.G. Fedorov, "Two phase convective cooling for ultra-high power dissipation in microprocessors," *Thermal and Thermomechanical Phenomena in Electronic Systems (ITherm), 2014 IEEE Intersociety Conference on* , vol., no., pp.199,204, 27-30 May 2014.
4. V. Hatty, H. Kahn, A.H. Heuer, "Fracture Toughness, Fracture Strength, and Stress Corrosion Cracking of Silicon Dioxide Thin Films," *Microelectromechanical Systems, Journal of* , vol.17, no.4, pp.943,947, Aug. 2008
5. Xiangzhao, Ye-Yuming, Sun-Fujiang, Tu-Yunhua, Liusang,, "Crack growth analysis of ball grid array resistor's solder joint subjected to thermal cycling and 4 point cycling bending," *Electronic Packaging Technology & High Density Packaging, 2008. ICEPT-HDP 2008. International Conference on* , vol., no., pp.1,4, 28-31 July 2008.
6. Chun-Chi Chiu, Yun-Tsung Li; Hsun-Fa Li; Chuei-Tang Wang, "Fine pitch BGA solder joint split in SMT process," *Microsystems, Packaging, Assembly and Circuits Technology Conference, 2009. IMPACT 2009. 4th International* , vol., no., pp.602,605, 21-23 Oct. 2009.

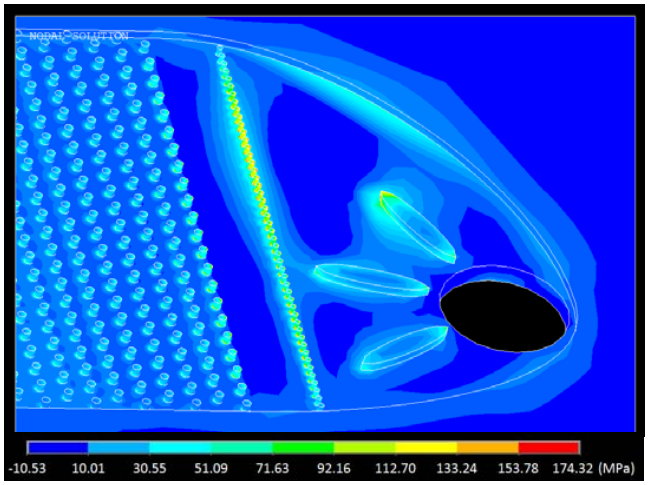

Fig. 12. Principal stress in silicon side for ideal bonding case